# Evaluation of Heat Treatments and Their Effects on the Corrosion Behavior of TiAlON Coatings Prepared by Cathodic Arc Evaporation on D3 Tool Steel

S. Shahabi[1], A. Shafyei[2][*] and M. A. Golozar[3]

*Department of Materials Engineering, Isfahan University of Technology, Isfahan, 84156-83111, Iran*

## Abstract

A series of TiAlON coatings were synthesized in a gaseous mixture of argon, nitrogen and oxygen by cathodic arc evaporation method using a Ti–Al mosaic target. Oxidation of coatings was carried out by heating the coated samples at the temperatures of 500, 600, 700, and 800°C for 1 h in air atmosphere. It was found that heat treatment changed the microstructure and composition of the coating. The dark copper color of TiAlON films was also changed due to the heat treatment. The peak intensities of TiN were decreased and that of Fe was increased with an increase in heat treatment temperature. Furthermore, the amorphous $Al_2O_3$ in grain boundaries was transformed to a crystalline structure with increasing temperature. The variation in the chemical composition of the coatings was recognized to be a function of heat treatment temperature. The oxidizing treatment promoted not only the growth of titanium and aluminum oxides on the pore wall of the coating, thereby allowing a partial pore sealing, but also the inter diffusion processes which increased the coating internal cohesion. The structure of TiAlON coatings was studied using X-ray diffraction (XRD) and scanning electron microscopy (SEM). Morphological characteristics were analyzed by means of an Atomic Force Microscopy (AFM). Corrosion resistance tests carried out in the 3.5%wt NaCl solution showed reduced corrosion current density due to the oxidation treatment. This post-coating treatment could be effective in improving the corrosion protection of TiAlON coating on a D3 substrate.

*Keywords:* Cathodic arc evaporation; TiAlON coating; Corrosion resistance; Heat treatment.

## 1. Introduction

Surface coating is an effective method to improve the durability of materials used in aggressive environments. Hard ceramic coatings, represented by TiN, have been extensively applied as cutting tool coatings with great achievements so far [1]. Researchers have claimed that it is possible to improve the properties of TiN coating by alloying it with other metals such as aluminum [2, 3], chromium [4], zirconium [5], and niobium [6] to form multi-component compound coatings. If the introduction of oxygen atoms into the TiAlN coating does not weaken the base material, TiAlON coating might be a good choice, because the formation of small amounts of oxides in the coatings can inhibit further oxidization [7]. The Ti–Al–N–O phase diagram shows a wealth of different structures, e.g., $Ti_xO_y$, $Ti_xN_y$, $Al_xN_y$, $Al_xO_y$, $Al_xTi_y$, and $Al_xTi_yN_z$, most of which exist in several polytypes [8]. In the PVD process, deposited oxide phases show an amorphous and thermally unstable state. High thermal loads, as in dry machining, cause the transformation of amorphous $Al_2O_3$ to crystalline θ-$Al_2O_3$ and α-$Al_2O_3$ [9].

It has been shown that (Ti,Al)N coatings with no oxygen have a columnar structure. As oxygen is introduced into the process, a similar columnar structure with a cubic-phase (Ti, Al)(O,N) solid solution is formed. Unlike (Ti,Al)N, the solid solution layer eventually becomes overgrown by a nanocomposite layer through renucleation, phase transformation, and competitive growth of nanocrystallites and amorphous phases of TiON, $TiO_2$, TiN, $Al_2O_3$, and AlN [8, 10].

Coating porosity and microstructure are characteristic features of these coatings and useful in corrosion resistance applications [11, 12]. Several ways have been proposed to reduce porosity and modify the structure. These include increasing coating thickness, controlling the bias potential during film deposition, multilayering and modifying film structure by heat treatment, and optimizing deposition parameters [1, 13].

In the present paper, an air furnace oxidation process was used as a post-coating treatment for both reducing the porosity and modifying the structure of TiAlON coatings obtained on AISI D3 tool steel substrate. The corrosion resistance characteristics of the coated and oxidized samples were evaluated and compared with those of as deposited ones.

* *Corresponding author:*
*Tel: +98 311 3915740      Fax: +98 311 3912752*
*Email: shafyei@cc.iut.ac.ir*
*Address: Department of Materials Engineering, Isfahan University of Technology, Isfahan, 84156-83111, Iran*
1. M.Sc.
2. Associate Professor
3. Professor

## 2. Experimental details

Coatings of TiAlON were deposited on an AISI D3 tool steel disk (diameter: 10 mm; thickness: 9 mm) using the cathodic arc deposition technique in a reactive atmosphere. The chemical composition of the D3 tool steel substrate is given in Table 1. Prior to the coating process, the specimens were heat treated to a hardness of 61 HRC. The heat treatment process involved austenitizing at 950°C for 60 min and quenching in oil, which was followed by tempering at 250°C for 60 min.

*Table 1. Chemical Composition of D3 Substrate steel .*

|    | C   | Si   | Mn   | Cr   | S     | Fe   |
|----|-----|------|------|------|-------|------|
| D3 | 1.2 | 0.35 | 0.30 | 12.5 | 0.010 | Bal. |

The coating thickness was measured by SEM technique using fractured cross section of the coated samples. The measured value of the coating thickness was approximately 2.7 μm. A Ti–Al mosaic target was made up of a 99.99% pure titanium target and 99.99% pure aluminum wires. A set of 30 holes with the identical diameter of 4.5 mm was drilled at high sputtering rate areas of the target into which the wires were subsequently inserted (Figure 1). The post-coating oxidation treatment was carried out in an air furnace at 500, 600, 700, and 800°C for 1 h.
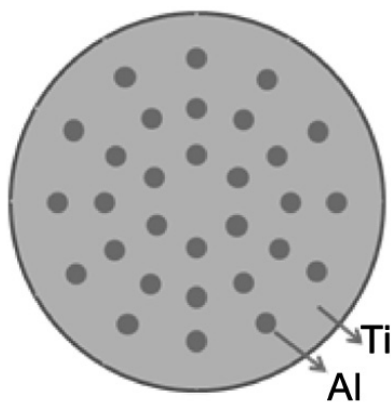


*Fig. 1. Ti–Al mosaic target with a surface ratio of 90.5/9.5.*

The microstructures of the coated samples were examined by atomic force microscope (AFM), SEM and energy dispersion spectroscopy (EDS) analysis techniques. X-ray diffraction analysis (Cu Kα radiation) was performed to identify the phases present in the surface layers.

In order to evaluate the corrosion behavior of the coatings, potentiodynamic polarization test measurements were conducted in an aerated 3.5 wt.% NaCl solution at room temperature. Test specimens were connected to a working electrode, and two high-purity graphite rods and a saturated calomel electrode

(SCE) were used as counter and reference electrodes, respectively. The exposed surface area of all the specimens was fixed at 1.4 cm², except the exposed area. Nitrocellulose polymer was used for painting the coating surface.

## 3. Results and discussion
### 3.1. Color changes due to heat treatment

The dark copper color of the as-deposited TiAlON films was changed due to heat treatment. Table 2 shows color variations observed. Color variations of TiAlON films could be attributed primarily to the existence of $TiO_2$ on the TiAlON film surface. The driving force of oxidation must be the Gibbs free energy change for TiN and $TiO_2$ [14]. Furthermore, as oxygen replaced nitrogen in the nitrides, oxygen behaved as if it were nitrogen, consuming the d-orbital electrons from the Ti metal. Thus, less light was reflected from the TiAlON film [15]. As a result, the films were changed from the dark copper to a blue-grey color with increasing temperature.

*Table 2. Film color changes due to heat treatment*

| Temperature | No heat treatment | 500°C | 600°C | 700°C | 800°C |
|-------------|-------------------|-------|-------|-------|-------|
| Color | Dark copper | Light brown | Blue | Dark yellow | Blue-gray |

### 3.2. XRD and SEM–EDS analyses

Figure 2 shows diffraction patterns for TiN films as-deposited and heat treated at 500, 600, 700, and 800°C for 1 h. High intensity diffraction peaks of TiN, AlN, $Al_2O_3$ and Fe (substrate) were detected in the scattering range of 2θ=20–90° for the as-deposited TiAlON film. While the peak intensities of TiN were decreased, the intensities of Fe were increased by increasing the heat treatment temperature. After heat treatment at 600 °C, the rutile structure $TiO_2$ phase could be detected. In addition, the peak of the $Fe_2O_3$ phase appeared after heat treatment at 800 °C. The width of the TiN peaks became narrower due to the heat treatment. This was explained by stress relief or grain growth of the coating as a result of increasing temperature [16].

Results from XRD showed the presence of amorphous $Al_2O_3$ in the coating. This amorphous structure phase was transformed to a crystalline structure phase when the heat treatment temperature was increased.

The oxidation behavior of TiAlON was mainly controlled by its Al and $Al_2O_3$ content. It has been reported that Al forms an amorphous aluminum oxide surface layer which causes the oxygen diffusion through the film to become more difficult. Detection of this amorphous layer was not possible by XRD. Furthermore, Al was diffused outward to the surface and oxygen was diffused into the film.

The superior oxidation behavior of TiAlON was also possibly due to the strongly differing values of Gibbs free energy for oxide formation. Over a wide temperature range, $Al_2O_3$ was much more stable than $TiO_2$ (i.e. for $Al_2O_3$, $\Delta G_\circ = -954$ kJ/mol and for $TiO_2$, $\Delta G_\circ = -756$ kJ/mol; both values were for 500°C and per mole of $O_2$) [17].
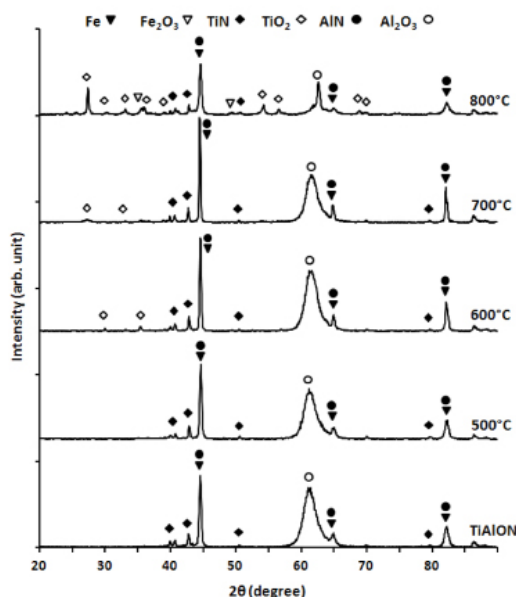


Fig. 2. XRD patterns of the TiN coating after heat treatment at different temperatures.

EDS analysis results indicated that the changes in the chemical composition of films were related to heat treatment. Table 3 and Figure 3 show approximate quantitative values obtained from EDS.

Table 3. Approximate quantitative values obtained from EDS analysis.

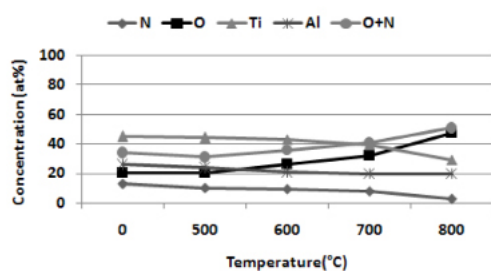| Heat treatment temperature | N at% | O at% | Al at% | Ti at% |
|---|---|---|---|---|
| As-deposited | 13.38 | 20.62 | 26 | 45 |
| 500°C | 10.33 | 20.77 | 23.79 | 44.23 |
| 600°C | 9.5 | 26.5 | 21 | 43 |
| 700°C | 8.31 | 32.32 | 19.8 | 39.55 |
| 800°C | 3.13 | 47.82 | 19.71 | 29.31 |



Fig.3. Surface atomic composition of TiAlON coating obtained from EDS after oxidation at different temperatures.

It was found that the N content was decreased as a result of increased heating temperature while the O content was increased. It is believed that N atoms are progressively substituted by O atoms. However, by increasing the temperature, the sum of these two elements is increased only slightly. Furthermore, one observes that the Al composition remains almost constant up to a temperature of 800 °C, which can be explained by Al out-diffusion as the main oxidation mechanism.

The amorphous $Al_2O_3$ in the grain boundary has a very important effect on the oxidation resistance of the coating [2, 8]. Indeed, the $Al_2O_3$ has been shown to decrease the atomic diffusivity in the coating [18].

As can be seen in Fig. 4, the surface morphology of TiAlON films was affected by heat treatment, while the TiAlON coating surface was generally smooth before heat treatment and its roughness was increased with increasing the temperature of the heat treatment.

The particles shown in Figure 4 are the liquid or solid debris produced at cathode spots. It is believed that the particles are formed through the action of plasma pressure on the melted cathode material present between the dense plasma and the relatively cold cathode body. The production of particles is, therefore, inherently connected to the existence of non-stationary cathode spots.

The macro-particles deposited in the early stage of the process can affect the oxidation resistance of the TiAlON coating in two ways. First, they are loosely adhered onto the underlying TiN-rich coating which is then exposed once the macro-particles are removed. Second, they may produce a shading effect which affects the deposition of subsequent layers of ions, resulting in microholes around the macro-particles. As TiN has a lower oxidation resistance, the oxidation resistance of the TiAlON coating will be reduced due to the defects created.

The SEM micrographs showed that the coating remained stable with no severe oxidation or micro-cracks appearing on the surface until a temperature of up to 800°C was reached. As a result, an Al-rich oxide layer was formed on the surface, slowing down the oxidation of the coating.

### 3.3. AFM analyses

Typical AFM images of as-deposited and heat treated TiAlON films are shown in Figure 5. Clearly, it can be observed that not only micro-cracks were developed, but also the good adhesion of the film was also observed while oxidation occurred at different temperatures. However, ompared to the as-deposited coating, roughness was increased. The Rms and Ra roughness of the coatings before and after heat treatment are shown in Figure 6.

The thermal process at 500°C reduced the roughness of the samples. Increasing the oxidation temperature, however, increased the coating roughness.

The increase in the Rms and Ra roughness is believed to be due to the formation of oxides on the film surface, which can have a higher molar volume than the nitride films [17].
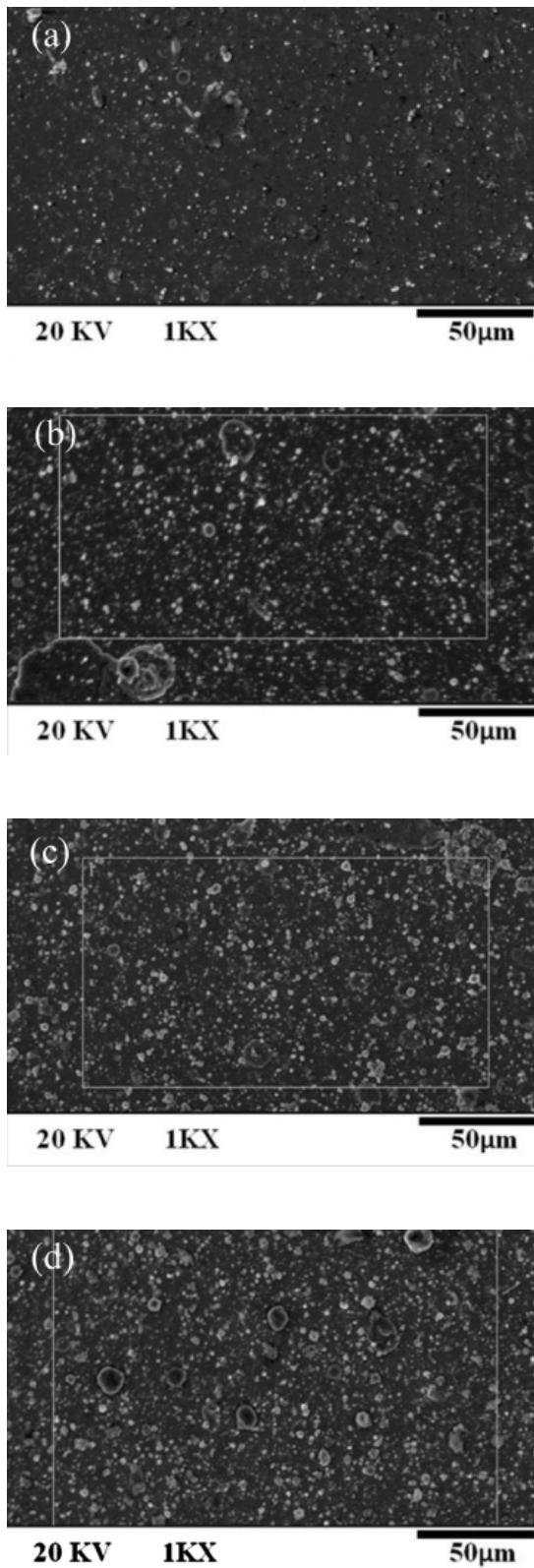


*Fig. 4. SEM micrographs of TiAlON coatings, (a) as-deposited and after oxidation in air for 1h (b) at 600°C, (c) at 700°C, and (d) at 800°C.*
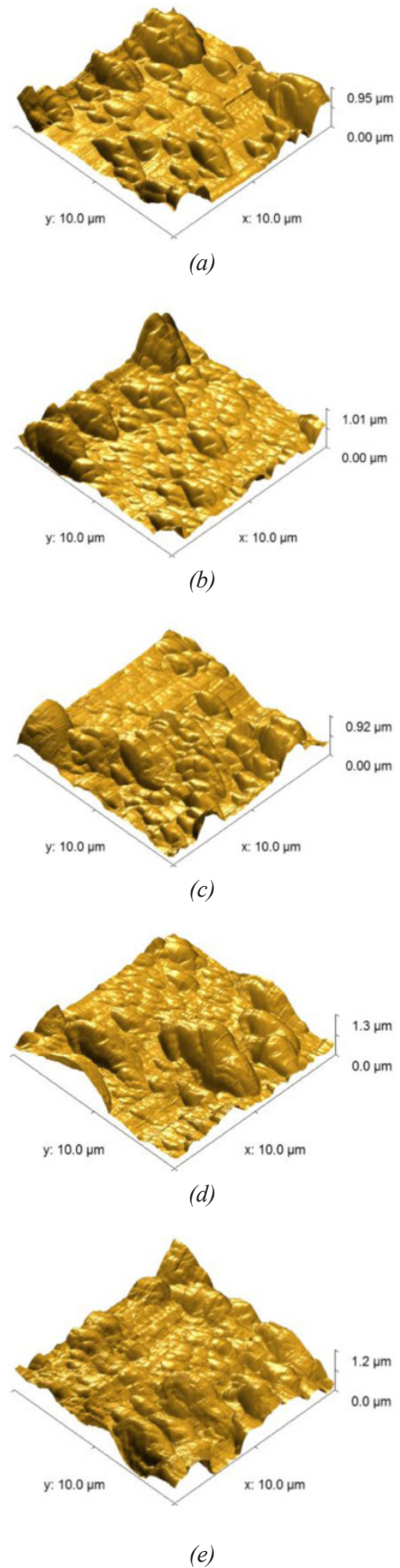


*Fig. 5. Three-dimensional AFM images of: (a) as-coated TiAlON and after oxidation in air for 1h (b) at 500°C, (c) at 600°C, (d) at 700°C, and (e) at 800°C.*
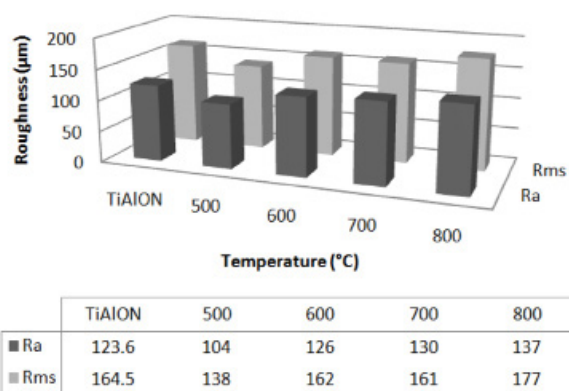
*Fig. 6. Variation in roughness with increasing oxidation temperature.*

## 3.4. Corrosion behavior

Corrosion tests were performed on the coated oxidized samples in 3.5%wt. NaCl solutions. As a reference, the test was also carried out on the as-coated sample with no oxidation. The typical polarization curves obtained are shown in Figure 7 and current density values calculated from Tafel extrapolation are listed in Table 4.

The corrosion current density and the corrosion potential were obtained from the intersection of the extrapolation of anodic and cathodic Tafel zones.

The corrosion current densities of the films after oxidation were much lower than those of the as-coated (with no oxidation). The films after oxidation at 600 and 700°C showed the lowest corrosion current density, indicating the lowest corrosion rate.

After the post-coating treatment, the cathodic current values were decreased further under the experimental conditions environment. In comparison with the as-coated samples, the corrosion current densities were decreased from 3.8 to 0.7 $\mu A$ cm$^{-2}$ in 3.5%wt. NaCl solution.

The PVD coatings contain cracks, pinholes, and pores which allow the corrosive media to enter and reach the substrate, thus degrading the corrosion behavior of the coating/substrate system.

During the chemical attack, Al would be easily transformed to $Al_2O_3$ on the surface of the coating, thereby passivating the surface and preventing further corrosion attacks. Indeed, the presence of a passive layer leads to additional resistance to the corrosive medium passing through the pores [19].

Since the titanium and aluminum oxides formed during the oxidation process tend to partially seal the coating pores, further transformation of amorphous $Al_2O_3$ to crystalline $Al_2O_3$ at grain boundary enhances the corrosion resistance of TiAlON coatings.

## 4. Conclusions

The TiAlON film was deposited from a Ti-Al mosaic target using the cathodic arc deposition technique.

The oxidation experiments indicated that TiAlON film was oxidized to $TiO_2$ when the oxidation temperature was above 600°C. The amorphous $Al_2O_3$ was also transformed to crystalline $Al_2O_3$ at 800°C. The amorphous $Al_2O_3$ enhanced the oxidation resistance of TiAlON coatings. A post-coating air oxidation process was proposed in order to improve the corrosion resistance properties of the TiAlON coating. The treatment (at 500°C to 800°C for 1 h) induced partial sealing of the coating's pores by means of titanium and aluminum oxide growth. Polarization tests performed in 3.5%wt. NaCl solution showed that upon immersion in an aggressive electrolyte and after oxidation, the tested TiAlON coatings, as compared to the as-deposited counterparts, exhibited a marked decrease in their corrosion current density.
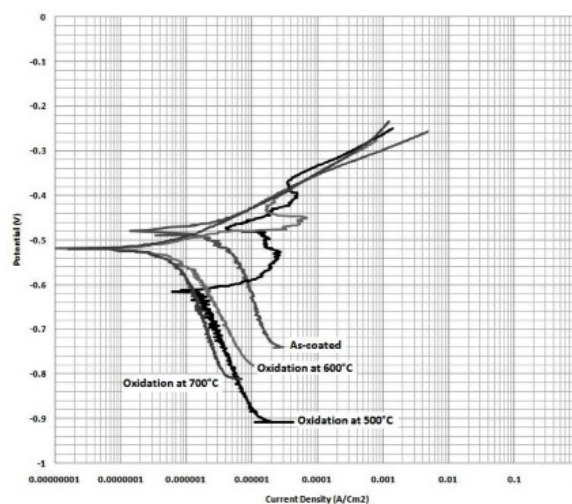


*Fig. 7. Polarization curves of the as-coated as well as coated and oxidized samples tested in 3.5%wt. NaCl solutions.*

*Table 4. Corrosion data extracted from polarization curves in Figure 7.*

| Coating | E corr (mv) | I corr (μA) | β an (mv) | βca (mv) |
|---|---|---|---|---|
| As-coated | -459 | 3.8 | 395 | 75 |
| Heat treated at 500°C | -614 | 1.7 | 350 | 26 |
| Heat treated at 600°C | -500 | 0.8 | 270 | 31 |
| Heat treated at 700°C | -508 | 0.7 | 452 | 71 |

## References

[1]  W. J.  Chou, G.P. Yu and J. H. Huang:  Corros. Sci., 43(2001), 2023.

[2]   S. PalDey and SC. Deevi: Mater. Sci. Eng., 342(2003), 58.

[3]   J. Musil and H. Hruby, Thin Solid Films., 365(2000), 104.

[4]  A. Kimura, H. Hasegawa, K. Yamada and TJ. Suzuki: Sci. Lett., 19(2000), 601.

[5]  J. Vetter, HJ. Scholl and O. Knotek: Surf. Coat. Technol. 74-75 (1995), 286.

[6]  I. Grimberg, VM. Zhitomirsky, RL. Boxman, S. Goldsmith and BZ. Weiss: Surf. Coat. Technol., 108-109(1998), 154.

[7]  L. Yan, Y. Dong, W. Zhao and G. Li: Int. J. Refract. Met. Hard. Mater., 25 (2007), 271.

[8]   J. Sjölén, L. Karlsson, S. Braun, R. Murdey, A. Hörling and L. Hultman: Surf. Coat. Technol. 201(2007), 6392.

[9]  K. Tonshoff, B. Karpuschewski, A. Mohlfeld, T. Leyendecker, G. Erkens, H.G. Fub and R. Wenke: Surf. Coat. Technol., 108–109(1998), 535.

[10]  S.B. Sant and K.S. Gill: Surf. Coat. Technol., 68(1994), 152.

[11]  C. H. Hsu, M. L. Chen and K.L. Lai: Mater. Sci. Eng. A., 421(2006), 182.

[12]  X.Z. Ding, X.T. Zeng, Y.C. Liu, L.R. Zhao and J. Vac: J. Vac. Sci. Technol. A., 24(2006), 974.

[13]  B.F. Chen, W.L. Pan b, G.P. Yu, J. Hwang and J.H. Huang: Surf. Coat. Technol., 111(1999), 16.

[14]  L. Fu-Hsing, F. Shiaw-Pyng, C. Hong-Ying and L. Ji-Kwei: Thin Solid Films.,375 (2000), 123.

[15]   S. Niyomsoan, W. Grant, D.L. Olson and B. Mishra: Thin Solid Films., 415 (2002), 187.

[16]  A. Mubarak, E. Hamzahand and M. R. M. Toff: Jurnal Mekanikal, 20(2005), 42.

[17]  C. Harish Barshilia, M. Surya Prakash, Anjana Jain and K.S. Rajam: Vacuum 77(2005), 169.

[18]  J.L. Huang and B.Y. Shew: J. Am. Ceram. Soc., 82(1999), 696.

[19] V.K. William Grips, H. C. Barshilia, V. EzhilSelvi, Kalavati and K.S. Rajam: Thin Solid Films 514(2006), 204.